IIETA International Information and Engineering Technology Association
Advancing the World of Information and Engineering

Mathematical Modelling of Engineering Problems
Vol. 13, No. 2, February, 2026, pp. 235-243
Journal homepage: http://iieta.org/journals/mmep

Rapid and Non-Invasive Detection of Chronic Kidney Disease via Urine-Based Raman Spectroscopy

Zeyad Al-Ibadi[1*], Hussein Neama Najeeb[1], Mohammed Ridha Janabi[1], Ban Salam Abdalhadi[2], Sajjad Abbas Hadi Nukhailawi[1], Zainab Nadhim Abdul Kadhim Mahdi[1]

[1] Department of Laser Physics, College of Science for Women, University of Babylon, Hillah 51001, Iraq
[2] Department of Radiology, College of Health and Medical Technology, University of Hilla, Hillah 51001, Iraq

Corresponding Author Email: wsci.ziead.khalaf@uobabylon.edu.iq

https://doi.org/10.18280/mmep.130201

Received: 18 October 2025
Revised: 20 December 2025
Accepted: 30 December 2025
Available online: 15 March 2026

Keywords:
Raman spectroscopy, urine analysis, kidney disease, spectral biomarkers, non-invasive diagnosis, multivariate analysis

ABSTRACT

Chronic kidney disease (CKD) is a global health problem that often progresses silently and remains undiagnosed in its early stages when using conventional biochemical tests. This study explores a non-invasive spectroscopic method for the early detection of CKD through urine analysis using Raman spectroscopy. Urine samples were collected from 50 patients diagnosed with CKD and 50 clinically healthy volunteers. The processed spectra were analyzed with particular attention to 8 characteristic Raman peaks at 620, 720, 825, 1002, 1180, 1450, 1550, and 1650 cm^{-1}. Principal component analysis, linear discriminant analysis, and support vector machine models are statistical and machine learning classification techniques that were used to differentiate disease and healthy cohorts. The most salient intensity differences were found at 1002 cm^{-1} and 1450 cm^{-1} spectral intensity peaks ($p < 0.001$). The region under the receiver operating characteristic curve of the 1002 cm^{-1} 1002 cm^{-1} peak was about 0.869 that indicates a strong discriminatory power. Linear discriminant analysis was applied with a primary diagnostic model that had a confirmed classification accuracy of 93.3, and sensitivity and specificity of 94 and 80, respectively. These findings suggest that urine Raman spectroscopy provides a rapid and cost-effective approach for detecting early kidney dysfunction, particularly in community-based and resource-limited healthcare settings.

1. INTRODUCTION

Chronic kidney disease (CKD) is an international health problem and a leading cause of morbidity and mortality, with over one out of ten adults being affected. Renal dysfunction should be identified at an early stage before it becomes inevitable and irreversible by the loss of the majority of nephrons, to avoid the burden put on the social and financial health of the patient induced by dialysis or kidney transplants.

In third-world countries, particularly in Iraq, such a shortage of expedient, rapid, and reliable diagnostic tools hinders effective screening and longitudinal control of renal pathologies [1, 2].

The current diagnostic modalities that are in use, which are mainly invasive methods, are serum urea and creatinine assays, ultrasonography, and rapid urine screening tests. These techniques are not only restricted by the invasive aspect, but they also have a long processing time and may require highly advanced, state-of-the-art equipment, which is not always available in resource-limited environments.

The constraints listed above have stimulated the research activities aimed at the creation of optical and molecular approaches that would be able to detect the biochemical changes that are in advance of the patient developing chronic kidney disease [3, 4].

Failure of traditional diagnostics has led to the consideration of alternative diagnostic models, especially optical and molecular models that have the ability to detect minor alterations in the biochemistry of body fluids. Raman spectroscopy has taken the centre stage in this regard as it has become one of the promising techniques of analysis, a label-free, non-destructive method to explain the molecular fingerprints of a biofluid like urine.

Specific molecular information on proteins, lipids, and metabolites that are subject to drastic changes in renal disease is available through Raman spectral analysis, which provides early notifications of disease before clinical manifestation and observable serum changes [5, 6].

Recent studies have demonstrated the potential of vibrational spectroscopy, including Raman, Fourier transform infrared (FTIR) spectroscopy, and surface-enhanced Raman scattering (SERS), in identifying spectral biomarkers of kidney disease. For example, Raman spectra of urine can distinguish patients with CKD from healthy controls with a diagnostic accuracy above 95% [3, 7]. Similarly, SERS spectra from serum and urine can be used to detect CKD with high sensitivity [6, 8]. Clear spectral differences between urine samples from end-stage renal disease patients and healthy individuals have been reported [9].

Further studies have explored the quantification of

creatinine and urea using Raman and FTIR spectroscopy [4], and spectral variations linked to diabetic kidney disease or glomerulonephritis have been verified in recent studies [5, 6]. The integration of multivariate and machine-learning algorithms, such as principal component analysis (PCA), linear discriminant analysis (LDA), support vector machine (SVM), and Random Forest, has enhanced classification performance in spectroscopic renal diagnostics [7-9].

The literature reviews confirm that near-infrared spectroscopy, mid-infrared spectroscopy, and Raman modalities are being considered more useful as non-invasive methods of detecting and longitudinally tracking renal pathologies [7, 10]. Therefore, the present study aims to evaluate the diagnostic potential of urine-based Raman spectroscopy as a rapid, cost-effective, and non-invasive approach for early detection of kidney diseases.

The study compares Raman spectral fingerprints of urine samples of people who are clinically healthy and patients with renal disease. It determines typical spectral biomarkers differentiating two groups of patients and measures diagnostic performance using multivariate statistical modeling in a community-based healthcare system [11, 12].

2. METHODOLOGY

This study conducted an observational case-control analysis to compare urine samples from healthy individuals and patients with renal disorders. The methodology involved five key stages, including analysis of the specimen, spectroscopic measurement, preprocessing of the data, statistical modelling, and validation of the modelling strategy [13-16].

2.1 Sample collection and storage

A total of 100 morning urine samples were collected, including 50 samples from clinically healthy volunteers and 50 patients. The sample of patients comprised patients with chronic disease and a CKD history as per the hospital medical records before enrollment.

Samples were collected in sterile containers and subsequently subjected to Raman spectroscopic analysis. (Figure 1) presents the processed Raman spectra of healthy and diseased samples. Samples were immediately kept at 4 ℃ to inhibit enzymatic activity and prevent the growth of microorganisms.

According to standard practice, urine samples intended for biochemical or spectroscopic analysis can be stored at 4 ℃ for up to 24 hours without significant deterioration of molecular components detectable by Raman spectroscopy [1, 4, 17].

2.2 Spectral data acquisition

A portable Raman spectrometer was used to obtain spectra at an excitation wavelength of 785 nm. The spectrometer had a spectral coverage of 400–1800 cm^{-1} and a resolution of the instrument of less than 5 cm^{-1}. Exposure parameters were set at 10s per acquisition, and the mean intensity was calculated based on three independent measurements on each sample, to reduce the inter-sample variation and increase the signal-to-noise ratio. The incident power of the laser was adjusted to about 100 mW, so that the sample was not damaged by the photodegradation of the laser signal [18].

2.3 Spectral preprocessing

A general preprocessing model was used to maximise the quality of the original spectra. Various methods were combined in the workflow, such as the correction of the baselines, Savitzky-Golay filtering to smooth the data, and median filtering to remove the noise, which was finished with a normalisation step.

The strict methodology was used so that all spectral features could be compared and artifact-free, thus providing a stable platform to work on further analysis [6, 7].

In Figure 1, 50 spectra of the processed healthy samples are shown in the upper panel, whereas 50 spectra of the processed diseased samples are displayed in the lower panel.

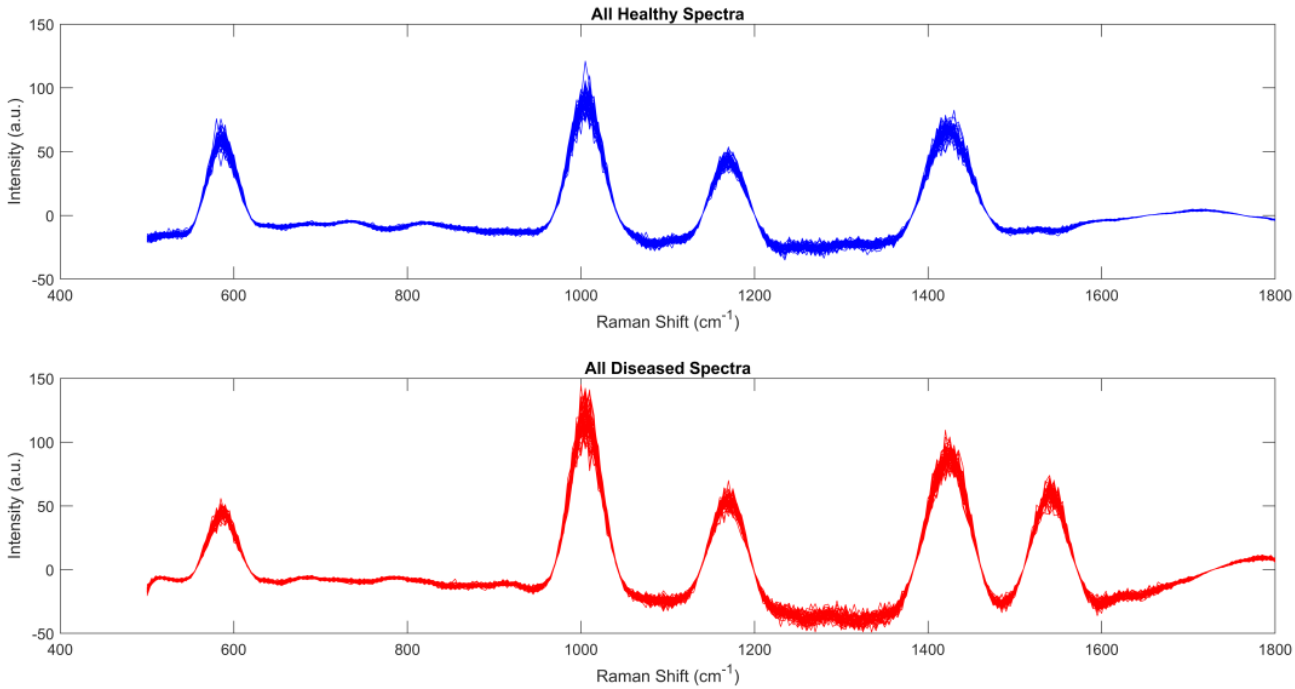

Figure 1. Processed Raman spectra of healthy and diseased samples

2.4 Statistical and multivariate analysis

In the present work, PCA was used to reduce the dimensionality of the data and present spectral variance. Based on previous Raman spectroscopic research indicating the presence of kidney-related biochemical markers in urine, eight distinct Raman peaks were selected for further investigation. Classification models were developed using LDA and the SVM algorithm to distinguish between healthy and diseased spectra. In this aspect, a training-to-validation split of 70:30 was employed to evaluate model generalizability [2, 19].

2.5 Model evaluation

There were four main diagnostic measures (classification accuracy, sensitivity, specificity, and area under the receiver operating characteristic curve (AUC)), which were used to evaluate 4- Model performance. A 10-fold cross-validation method has been used to assess the robustness of models as well as minimize overfitting in all models of classification. The metrics were determined in each of the folds and reported as the average of the values across folds.

Independent t-tests were used to calculate statistical differences between groups in spectral measurements, and $p < 0.001$ was considered the significance threshold [1, 4]. All data analysis and modeling were conducted using MATLAB R2019a, which included specific toolboxes for multivariate spectral analysis.

3. RESULTS AND DISCUSSION

3.1 Spectral characteristics and peak-level analysis

The urine sample in the spectroscopic analysis showed a statistically significant difference between the patients with CKD and the healthy controls, as shown in Figure 2. The Raman bands at 620, 825, 1002, 1180, 1450, 1550, and 1650 cm^{-1} exhibited notable intensity variations between groups [4, 17].

An increase in intensity of multiple such spectral positions in the CKD group is consistent with changes in protein metabolism, lipid-related structures, and compounds with nitrogen found in chronic kidney disease. A summary of molecular assignments and their clinical relevance is provided in Table 1 [1, 17].

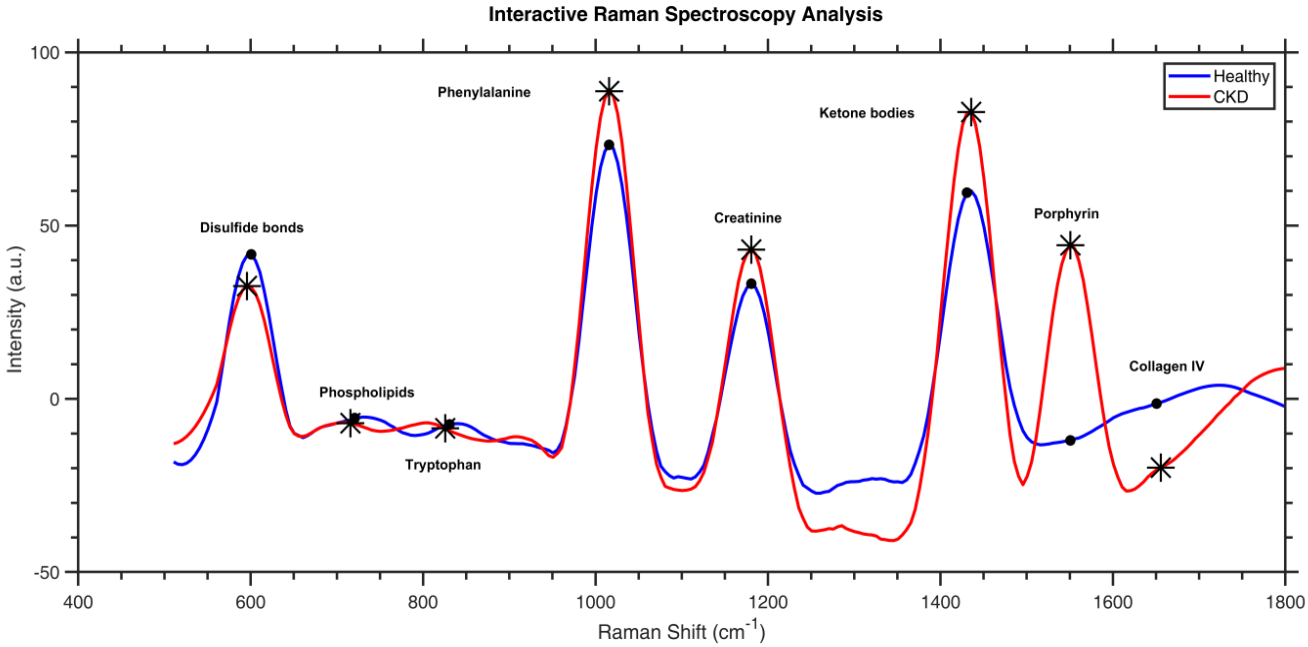

Figure 2. Typical Raman spectrum of urine of chronic kidney disease patients and healthy individuals with major biochemical peaks

Table 1. Refer to Raman spectral peaks and biochemical or clinical importance in kidney disease

Wavenumber (cm^{-1})	Associated Compound	Clinical Significance in Kidney Diseases
620	Carbon–sulfur (C–S) bonds in disulfides	Tubular damage + oxidative stress
720	Phospholipids from cell membranes	Tubular epithelial damage in chronic kidney disease
825	Indole ring in tryptophan	Active renal inflammation
1002	Phenylalanine (Benzene ring)	Glomerular damage (proteinuria)
1180	Carbon–nitrogen (C–N) vibrations	The reference is for muscle mass rather than kidney function, warranting careful interpretation.
1450	CH_2 groups in ketone bodies (β-hydroxybutyrate)	Metabolic renal acidosis
1550	Porphyrin from heme catabolism	Immune hematuria
1650	Amide I in Collagen IV	Renal fibrosis

Peak-wise evaluation indicated higher signals corresponding to phenylalanine (~1002 cm^{-1}), creatinine-related carbon–nitrogen (C–N) vibrations (~1180 cm^{-1}), ketone-associated bands (~1450 cm^{-1}), and porphyrin-related

structures (~1550 cm^{-1}) in CKD samples compared with controls [2]. Against previous findings, weaker intensity 1650 cm^{-1} demonstrated changes in the structural components of the protein, especially the amide I vibrations of the collagen [4].

The disulfide bond stretching vibrations can be observed at the absorption band of 620 cm^{-1} minus the reflection in the survey band (618–623 cm^{-1}). commonly associated with oxidized protein species in urine. Increased intensity at this band was linked to oxidative stress and renal tubular cellular injury [20].

The 720 cm^{-1} band (715–725 cm^{-1}) represents phosphate chain rocking and phospholipid-related structures, including phosphatidylcholine, and may reflect alterations in renal epithelial membrane integrity in CKD [17].

The 825 cm^{-1} band (822–828 cm^{-1}) corresponds to out-of-plane bending of tryptophan ring structures [1]. The 1002 cm^{-1} peak (1001.5 ± 0.7 cm^{-1}) is assigned to the symmetric ring breathing mode of phenylalanine. The 1180 cm^{-1} band (1178–1183 cm^{-1}) is attributed to C–N asymmetric stretching vibrations predominantly associated with creatinine.

The 1450 cm^{-1} band (1445–1455 cm^{-1}) reflects CH_2 scissoring vibrations and is commonly related to lipid and ketone-associated metabolites [4, 21]. The 1550 cm^{-1} band (1548–1553 cm^{-1}) corresponds to pyrrole ring stretching vibrations linked to porphyrin-related compounds [1, 22]. The 1650 cm^{-1} band (1647–1655 cm^{-1}) represents amide I (C = O stretching) vibrations associated with structural proteins such as collagen and fibronectin [4, 17, 23].

The diagnostic sensitivity of certain spectral bands, in particular at 1002 and 1650 cm^{-1} and 1002, across a range of pathologies in the kidney has been reported by prior Raman spectroscopy studies [24, 25]. These results render some validity to the clinical significance of the above-mentioned peaks in measuring renal disease.

In the present analysis, the use of PCA indicated that the first two components carried a variance larger than 50% of the overall variance, and it is therefore worth keeping in further analysis (Figure 3).

3.2 Classification results and diagnostic model performance

The statistical test showed that there were significant mean differences between patient and control cohorts, both in Raman spectral data and in biochemical profiles. The percentage of variance accounted by each principal component (PC) is presented as shown in Figure 3. The greatest percentage of variance was described by component 1, and the smaller percentage was described by PC5 to PC6, which described less than 15%.

Existence of an elbow implies that the total retention of the first two components is the best expression of the salient structure of the data without massive loss of information. These observations imply that the outcomes of the PCA indicate that the two components, PC1 and PC2 combined, explain over half of the entire variance, which proves that it will be eligible to use these two components in a two-dimensional display to make further analyses [5, 7, 11]. Table 2 provides a summary of a peak-level analysis, indicating the statistical significance and diagnostic performance indices related to each Raman band, which were tested independently based on their discriminative capability.

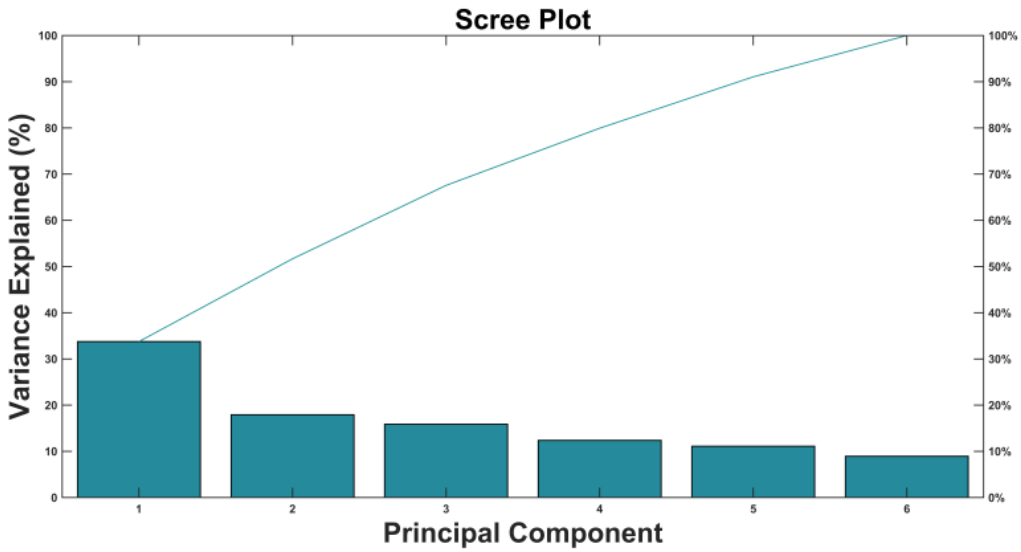

Figure 3. Scree plot with percent of variance due to each principal component

Table 2. Statistical values of important Raman spectral peaks related to kidney disease diagnosis

Raman Shaft (cm^{-1})	P Value	T Value	Accuracy	Specificity	Sensitivity	Threshold	Area Under the Receiver Operating Characteristic Curve
620	0.0301	2.41	0.64	0.60	0.68	41.20	0.6412
720	0.0125	3.85	0.71	0.66	0.76	51.00	0.7511
825	0.0233	2.69	0.66	0.62	0.70	60.70	0.6642
1002	0.0003	7.65	0.83	0.66	0.88	71.10	0.8690
1450	0.0007	5.98	0.80	0.92	0.58	83.00	0.7845
1650	0.0048	3.41	0.75	0.76	0.74	90.60	0.7650

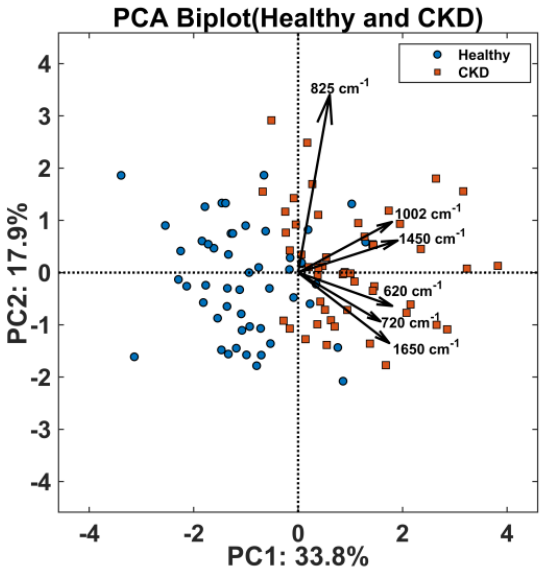

Figure 4. Principal components analysis (PCA) biplot of urine Raman spectra showing separation between healthy and chronic kidney disease (CKD) samples along PC1 (33.8%) and PC2 (17.9%)

Note: Loading vectors indicate the contribution of major Raman peaks (620–1650 cm^{-1}), with 1002 and 1450 cm^{-1} showing the strongest association with CKD samples.

Statistical metrics (p-values and t-values) are included to demonstrate the significance of spectral differences between the diseased and control groups, while diagnostic metrics (accuracy, sensitivity, specificity, and AUC) are reported to illustrate the individual capability of each Raman peak rather than to represent a complete diagnostic model.

The Raman band with diagnostic performance closest to it (maximum AUC of 0.8690) was identified at 1002 cm^{-1}, therefore, it has the potential to become a strong spectral biomarker. Other peaks at 720, 1450, and 1650 cm^{-1} minus were also performing well (AUC), which exceeded 0.75.

The PCA biplot (Figure 4) displays the separation of CKD and healthy urine samples using PC1 and PC2. Thus, close peaks are positively correlated, and opposite ones are negatively correlated. The projection of the samples onto PC1 (33.8%) and PC2 (17.9%), as a binary, indicates that the most significant variables in the determination of the difference between the samples were 620, 720, 825, 1002, 1450, and 1650 cm^{-1}.

The outcome of the PCA shows that spectral features with wavelengths 1002, 1450, and 1650 cm^{-1} play a significant role in the variance of disease to provide the differentiation of CKD samples compared to healthy samples. These results endorse the possibility of using these wavenumbers as spectral biomarkers in biospectral resources [22, 26]. Moreover, control samples that were healthy exhibited a more significant tendency to cluster around the lower-left quadrant of the PCA score plot. Even though some level of overlap among the groups was identified, the general distribution trend indicates that a desirable separability can be set out along the first two key elements (PC1 and PC2) [17, 19].

The biochemical identifications of the Raman bands are based on available literature and utilities of past spectral databases [2]. Although the bands at 1002 and 1450 cm^{-1} have frequently been associated with literature-based spectral assignments of phenylalanine and lipid/protein structure elements, respectively, they must also be taken to mean literature-based spectral assignments, as opposed to unequivocal biochemical assignments.

Figure 5 (PC boxplots) shows the distribution of the first three main components of the CKD and the healthy groups. Moreover, a significant deviation in the median (middle line) suggests that there is a difference between the two groups of people. The two groups have a distinct difference in the values of PC1 (first principal component), with CKD having higher values and healthy controls having lower values. The t-value (9.6026) was very large, and the p-value (8.8223×10^{-16}) was very small (well below 0.05), indicating that the difference between the two groups is very large. It can prove to be extremely useful as a diagnostic variable or within classification frameworks [22, 26].

However, PC2 and PC3 do not exhibit any statistically significant differences among participants in the two groups (p = 0.16545 and p = 0.18461, respectively) [8, 12].

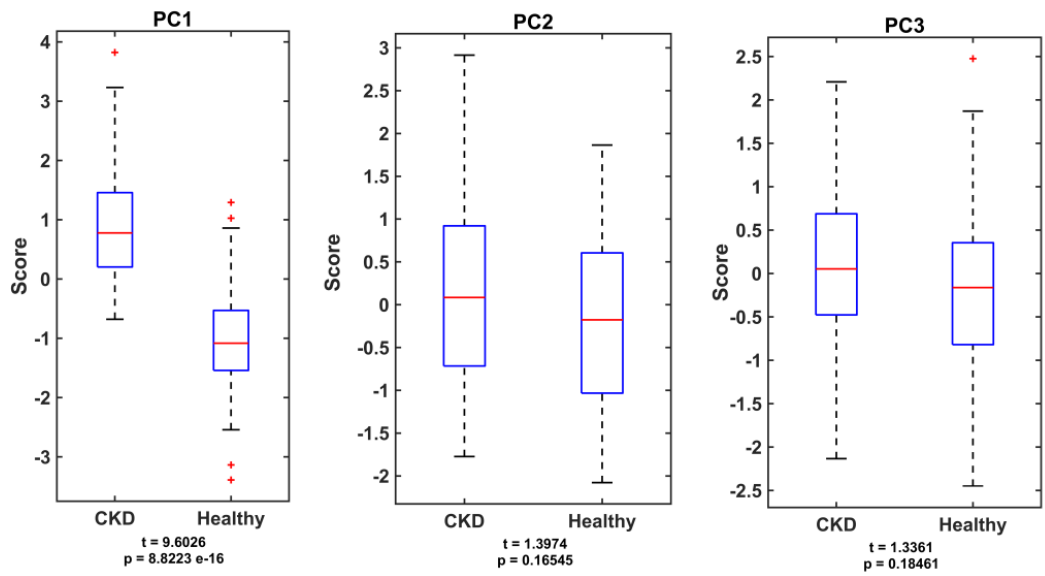

Figure 5. Boxplot of the first three principal components (PCs) scores of chronic kidney disease (CKD) patients and healthy subjects

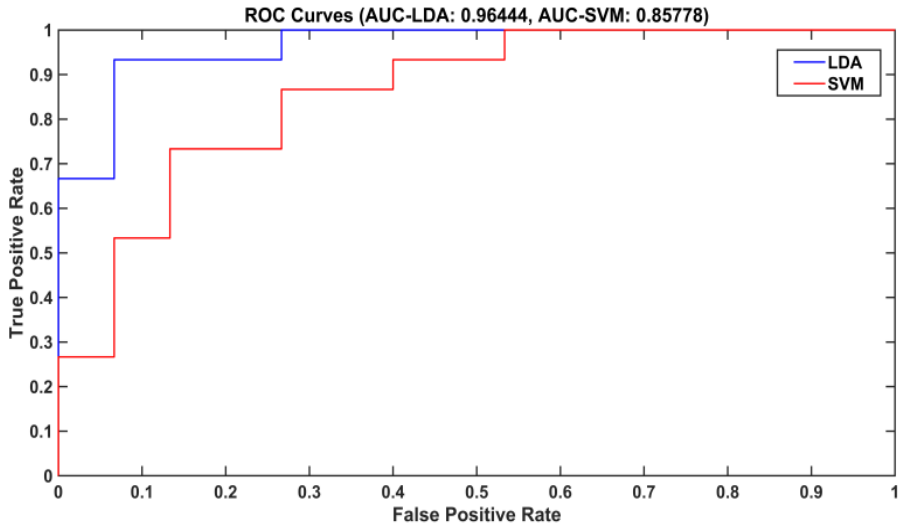

Figure 6. Receiver operating characteristic (ROC) curves on the classification of linear discriminant analysis (LDA) (blue) and support vector machine (SVM) (red) using full spectral features

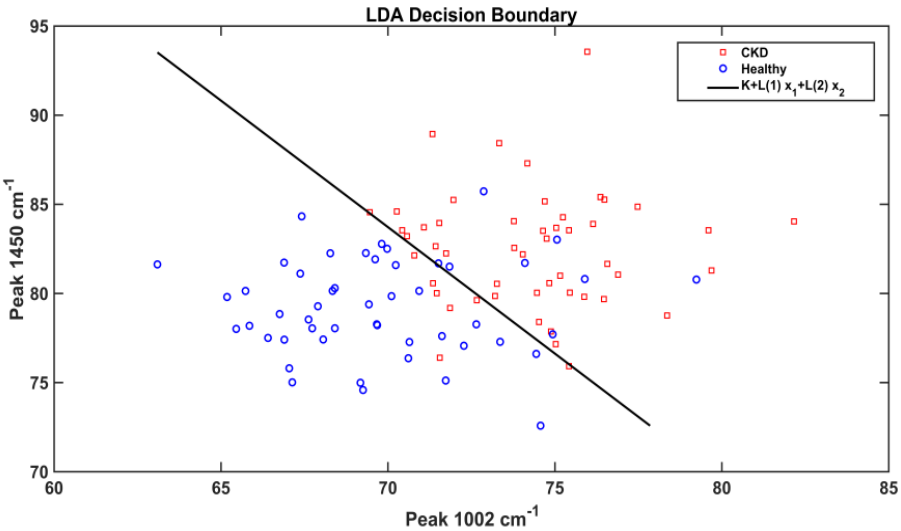

Figure 7. Linear discriminant analysis (LDA) classification diagram according to Raman peak intensities at 1002 cm^{-1} and 1450 cm^{-1} of chronic kidney disease (CKD) and healthy samples

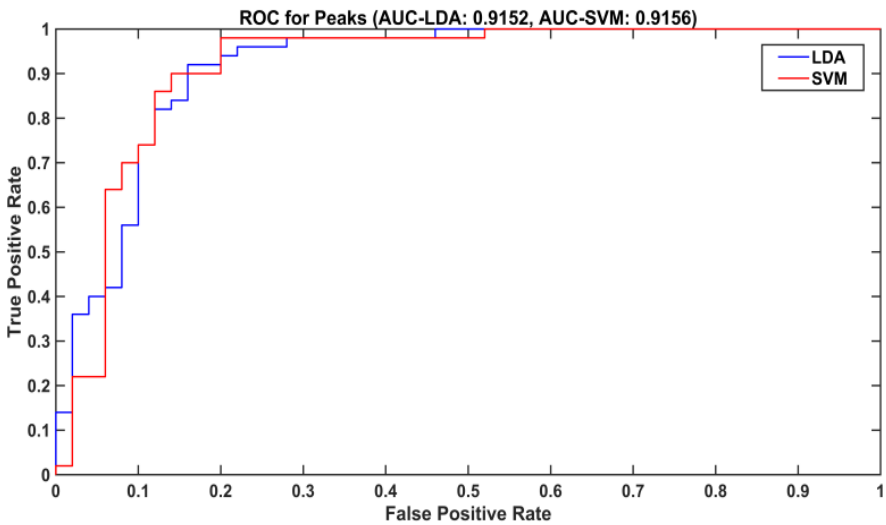

Figure 8. Receiver operating characteristic (ROC) curves for Linear discriminant analysis (LDA) (blue) and support vector machine (SVM) (red) classifiers using only selected spectral peak features

Figure 6 presents the receiver operating characteristic (ROC) curves comparing the performance of the LDA and SVM models in distinguishing CKD from healthy controls. Model performance is evaluated using the AUC, where a value of 0.5 indicates random classification and a value of 1.0 indicates perfect discrimination. In this study, AUC values exceeded 0.8, indicating good diagnostic performance, with values above 0.9 considered excellent.

The ROC curves indicate that the principal component-based model is clustered nearer to the upper-left corner, indicating a higher sensitivity and specificity. The LDA achieved an AUC 0.96444 greater than the SVM classifiers (AUC 0.85778), therefore indicating that it is a greater discriminative area in this data set. This difference suggests that the intergroup distinction is mainly straight, and LDA is a better method of analysis in the present study [8, 15].

Figure 7 displays an LDA decision boundary as calculated by using the spectral intensities of the most discriminative Raman peaks, requirements 1450, at 1002 cm^{-1} and 1450 cm^{-1}. The linear demarcation is used to indicate the SCKD samples, which are denoted by red squares, and healthy samples, which are denoted by blue circles. The samples of CKD are concentrated mainly in the upper-right region, indicating high levels of phenylalanine and porphyrin, whereas the samples of healthy people are concentrated in the lower-left sphere, which suggests the normal level of metabolites.

The clear separation achieved by the linear boundary highlights the diagnostic relevance of these spectral biomarkers [14, 25].

The ROC curves in Figure 8 consider the performance of LDA and SVM models built only using Raman peaks of 1002 cm^{-1} and 1450 cm^{-1}. The two spectral markers were adequate to differentiate the CKD patients and healthy controls. The values of the resulting AUC 0.9152 of LDA and 0.9156 of SVM are good diagnostic values and are comparable to the values derived using principal-component-based models (ROC- PCs).

Restricting the analysis to the most discriminative peaks reduced data dimensionality while preserving relevant classification information.

It is observed now that the used multifocal Raman spectral characteristics capture primary variance applicable to disease states.

The LDA model applied to the chosen Raman features was the major diagnostic model. This model had a total classification accuracy of 93.3%, sensitivity, and specificity of 94 and 80%, respectively, as described in the Model Evaluation section.

3.3 Comparison with previous Raman-based studies

Raman spectroscopy has been used in several studies that have reported excellent diagnostic ability of renal disorders with classification accuracy exceeding 95% in controlled experimental studies [1, 2]. However, many of these investigations were conducted on relatively small cohorts, under laboratory-controlled conditions, or using highly selective patient populations.

In the present study, urine samples were analyzed using a portable Raman spectrometer in a case-control study, and the AUC was discovered to fall within the range of 0.87 to 0.96 [13].

The values are less than some of the values obtained in some laboratory-based studies; however, they are allowed to be diagnostic and are more reflective of real-world screening scenarios.

The use of a mobile platform and the use of a heterogeneous clinical population are indicative of the practical limitations that are typically involved in community-based and resource-constrained healthcare environments.

It is therefore important to note that in comparing the diagnostic performance in the Raman-based studies, variations in study design, instrumentation, and cohort composition should be taken into consideration [21].

3.4 Novelty and contribution of the present study

This study addresses limitations observed in some Raman-based renal investigations, particularly the underexplored diagnostic contribution of specific spectral bands. The combined analytical relevance of the 1002 and 1450 cm^{-1} Raman peaks was evaluated within a multivariate modeling framework. Rather than considering these peaks independently, their joint contribution to classification performance was examined.

4. CONCLUSION

This study demonstrates the possibility of urinary analysis with Raman spectroscopy as a non-invasive mode of CKD detection. Detection of clear spectral characteristics at 1002 and 1450 cm^{-1} supports the targeted approach to assessing the effects of renal-associated biochemical changes.

This can be shown by the performance metrics: the LDA achieved 93.3% accuracy, compared to the SVM, which attained an AUC of 0.9156. These results demonstrate that diagnostically relevant spectral data can be obtained through multivariate modelling.

However, due to the pilot-based character of this research, further validation of such studies with large and multicentre cohorts is a precondition before introducing them in clinical practice.

Surveying reproducibility and standard spectral protocols will be an important means to apply the Raman-based diagnostics to the normal diagnostics of nephrology.

REFERENCES

[1] Ainiwaer, A., Sun, S.W., Bohetiyaer, A., Liu, Y.C., et al. (2025). Application of Raman spectroscopy in the non-invasive diagnosis of urological diseases via urine. Photodiagnosis and Photodynamic Therapy, 52: 104477. https://doi.org/10.1016/j.pdpdt.2025.104477

[2] Zong, M., Zhou, L., Guan, Q., Lin, D., Zhao, J., Qi, H., Harriman, D., Fan, L., Zeng, H., Du, C. (2021). Comparison of surface-enhanced Raman scattering properties of serum and urine for the detection of chronic kidney disease in patients. Applied Spectroscopy, 75(4): 412-421. https://doi.org/10.1177/0003702820966322

[3] Flores-Guerrero, J.L., Muñoz-Morales, A., Narea-Jimenez, F., Perez-Fuentes, R., Torres-Rasgado, E., Ruiz-Vivanco, G., Gonzalez-Viveros, N., Castro-Ramos, J. (2020). Novel assessment of urinary albumin excretion in Type 2 diabetes patients by Raman spectroscopy. Diagnostics, 10(3): 141. https://doi.org/10.3390/diagnostics10030141

[4] Kavuru, V., Senger, R.S., Robertson, J.L., Choudhury, D. (2023). Analysis of urine Raman spectra differences from patients with diabetes mellitus and renal pathologies. PeerJ, 11: e14879. http://doi.org/10.7717/peerj.14879

[5] Senger, R.S., Sullivan, M., Gouldin, A., Lundgren, S., et al. (2020). Spectral characteristics of urine from patients with end-stage kidney disease analyzed using Raman Chemometric Urinalysis (Rametrix). PLoS One, 15(1): e0227281. https://doi.org/10.1371/journal.pone.0227281

[6] Kong, X., Liang, H., An, W., Bai, S., Miao, Y., Qiang, J., Wang, H., Zhou, Y., Zhang, Q. (2023). Rapid identification of early renal damage in asymptomatic hyperuricemia patients based on urine Raman spectroscopy and bioinformatics analysis. Frontiers in Chemistry, 11: 1045697. https://doi.org/10.3389/fchem.2023.1045697

[7] Zhang, S., Ma, J., Qi, C., Cheng, R., Shen, J., Yang, H. (2025). Rapid detection of kidney disease based on urine surface-enhanced Raman spectroscopy and principal components analysis-support vector machine/random forests. Spectrochimica Acta Part A, Molecular and Biomolecular Spectroscopy, 343: 126492. https://doi.org/10.1016/j.saa.2025.126492

[8] Delrue, C., De Bruyne, S., Speeckaert, M.M. (2023) The potential use of near- and mid-infrared spectroscopy in kidney diseases. International Journal of Molecular Sciences, 24(7): 6740. https://doi.org/10.3390/ijms24076740

[9] Premasiri, W.R., Clarke, R.H., Womble, M.E. (2001). Urine analysis by laser Raman spectroscopy. Lasers in Surgery and Medicine, 28(4): 330-334. https://doi.org/10.1002/lsm.1058

[10] Senger, R.S., Issa, A.S., Agnor, B., Talty, J., Hollis, A., Robertson, J.L. (2022). Disease-associated multimolecular signature in the urine of patients with Lyme disease detected using Raman spectroscopy and chemometrics. Applied Spectroscopy, 76(3): 284-299. https://doi.org/10.1177/00037028211061769

[11] Senger, R.S., Sullivan, K.E., Maurer, K., Issa, A.S., Robertson, J.L. (2023). Identification of unique molecular "fingerprints" of Systemic Lupus Erythematosus (SLE) and evaluation of kidney function using urine Raman spectroscopy and chemometrics TH-PO793. Journal of the American Society of Nephrology, 34(11S): 311. https://doi.org/10.1681/ASN.20233411S1311a

[12] Siraj, N., Bwambok, D.K., Brady, P.N., Taylor, M., Baker, G.A., Bashiru, M., Macchi, S., Jalihal, A., Denmark, I., Le, T., Elzey, B., Pollard, D.A., Fakayode, S.O. (2021). Raman spectroscopy and multivariate regression analysis in biomedical research, medical diagnosis, and clinical analysis. Applied Spectroscopy Reviews, 56(8-10): 615-672. https://doi.org/10.1080/05704928.2021.1913744

[13] Lin, J., Huang, Z., Lin, X., Wu, Q., Quan, K., Cheng, Y., Zheng, M., Xu, J., Dai, Y., Qiu, H., Lin, D., Feng, S. (2020). Rapid and label-free urine test based on surface-enhanced Raman spectroscopy for the non-invasive detection of colorectal cancer at different stages. Biomedical Optics Express, 11(12): 7109-7119. http://doi.org/10.1364/BOE.406097

[14] Robertson, J.L., Senger, R.S., Talty, J., Du, P., Sayed-Issa, A., Avellar, M.L., Ngo, L.T., De La Espriella, M.G., Fazili, T.N., Jackson-Akers, J.Y., Guruli, G., Orlando, G. (2022). Alterations in the molecular composition of COVID-19 patient urine, detected using Raman spectroscopic/computational analysis. PLoS One, 17(7): e0270914. https://doi.org/10.1371/journal.pone.0270914

[15] Al-Zeyad, I., Alboedam, M., Katanov, I., Sura, A.Z. (2021). Detecting levels and innovative applications for the detection of aromatic compounds using multivariate curve analysis and spectroscopy data. NeuroQuantology, 19(3): 46-56. https://doi.org/10.14704/nq.2021.19.3.NQ21027

[16] Zeyad, A.I., Alboedam, M., Katanov, I., Sura, A.Z. (2021). Application of mathematical models and digital filters and their processors of spectral analysis for aromatic compounds gas in a fluorescent chemical. Turkish Journal of Computer and Mathematics Education, 12(5): 1148-1158. https://doi.org/10.22075/ijnaa.2021.4916

[17] Delrue, C., Speeckaert, M.M. (2022). The potential applications of Raman spectroscopy in kidney diseases. Journal of Personalized Medicine, 12(10): 1644. https://doi.org/10.3390/jpm12101644

[18] Stolpe, S., Kowall, B., Scholz, C., Stang, A., Blume, C. (2021). High unawareness of chronic kidney disease in Germany. International Journal of Environmental Research and Public Health, 18(22): 11752. https://doi.org/10.3390/ijerph182211752

[19] Zhao, N., Shi, P., Wang, Z., Sun, Z., Sun, K., Ye, C., Fu, L., Lin, C.T. (2024). Advances in surface-enhanced Raman spectroscopy for urinary metabolite analysis: Exploiting noble metal nanohybrids. Biosensors, 14(12): 564. https://doi.org/10.3390/bios14120564

[20] Saatkamp, C.J., de Almeida, M.L., Bispo, J.A.M., Pinheiro, A.L.B., Fernandes, A.B., Silveira Jr, L. (2016). Quantifying creatinine and urea in human urine through Raman spectroscopy aiming at diagnosis of kidney disease. Journal of Biomedical Optics, 21(3): 037001. https://doi.org/10.1117/1.JBO.21.3.037001

[21] Aitekenov, S., Sultangaziyev, A., Ilyas, A., Dyussupova, A., Boranova, A., Gaipov, A., Rostislav Bukasov, R. (2022). Surface-enhanced Raman spectroscopy (SERS) for protein determination in human urine. Sensing and Bio-Sensing Research, 38: 100535. https://doi.org/10.1016/j.sbsr.2022.100535

[22] Carswell, W., Robertson, J.L., Senger, R.S. (2022). Raman spectroscopic detection and quantification of macro-and microhematuria in human urine. Applied Spectroscopy, 76(3): 273-283. https://doi.org/10.1177/00037028211060853

[23] Zhang, X., Song, X., Li, W., Chen, C., Wusiman, M., Zhang, L., Zhang, J., Lu, J., Lu, C., Lv, X. (2023). Rapid diagnosis of membranous nephropathy based on serum and urine Raman spectroscopy combined with deep learning methods. Scientific Reports, 13: 3418. https://doi.org/10.1038/s41598-022-22204-1

[24] Zhu, G., Shadekejiang, H., Zhang, X., Chen, C., Su, M., Wu, S., Aimaijiang, G., Zhang, L., Wang, S., Yang, W., Lu, C. (2025). Rapid diagnosis of membranous nephropathy based on kidney tissue Raman spectroscopy and deep learning. Scientific Reports, 15: 13038. https://doi.org/10.1038/s41598-025-97351-2

[25] Movasaghi, Z., Rehman, S., Rehman, I.U. (2007). Raman spectroscopy of biological tissues. Applied Spectroscopy Reviews, 42(5): 493-541.

https://doi.org/10.1080/05704920701551530
[26] Huttanus, H.M., Vu, T., Guruli, G., Tracey, A., Carswell, W., Said, N., Du, P., Parkinson, B.G., Orlando, G., Robertson, J.L., Senger, R.S. (2020) Raman chemometric urinalysis (Rametrix) as a screen for bladder cancer. PLoS One, 15(8): e0237070. https://doi.org/10.1371/journal.pone.0237070